Plant, Cell & Environment

Plant, Cell and Environment (2012) **35**, 61–71 doi: 10.1111/j.1365-3040.2011.02428.x

Strategies of a Bornean tropical rainforest water use as a function of rainfall regime: isohydric or anisohydric?

TOMO'OMI KUMAGAI[1,2] & AMILCARE PORPORATO[2]

[1]Hydrospheric Atmospheric Research Center, Nagoya University, Furo-cho, Chikusa-ku, Nagoya, Japan and [2]Department of Civil and Environmental Engineering, Duke University, Durham, NC, USA

ABSTRACT

Although Bornean tropical rainforests are among the moistest biomes in the world, they sporadically experience periods of water stress. The observations indicate that these ecosystems tend to have little regulation of water use, despite episodes of relatively severe drought. This water-use behaviour is often referred to as anisohydric behaviour, as opposed to isohydric plants that regulate stomatal movement to prevent hydraulic failure. Although it is generally thought that anisohydric behaviour is an adaptation to more drought-prone habitats, we show that anisohydric plants may also be more favoured than isohydric plants under very moist environments where there is little risk of hydraulic failure. To explore this subject, we examined the advantages of isohydric and anisohydric species as a function of the hydroclimatic environment using a stochastic model of soil moisture and carbon assimilation dynamics parameterized by field observations. The results showed that under very moist conditions, anisohydric species tend to have higher productivity than isohydric plants, despite the fact that the two plant types show almost the same drought-induced mortality. As precipitation decreases, the mortality of anisohydric plants drastically increases whereas that of isohydric plants remains relatively constant and low; in these conditions, isohydric plants surpass anisohydric plants in their productivity.

Key-words: climate change; drought; mortality; photosynthesis; plant water stress; soil water balance; stochastic process; transpiration.

INTRODUCTION

Tropical forests in Southeast Asia represent approximately 11% of the world's tropical forests in terms of area (World Resources Institute 2007). These forests have the highest relative deforestation rate among all forests in tropical areas (Houghton & Hackler 1999; Malhi & Grace 2000), and their possible roles in the global and regional climate and hydrological cycles are important concerns (e.g. Kanae, Oki & Musiake, 2001; Malhi & Wright 2004; Mabuchi, Sato & Kida 2005; Werth & Avissar 2005). An analysis of climatic trends of global tropical rainforest regions showed that rainfall appears to have declined more significantly in Southeast Asia than in Amazonia, and that the El Niño Southern Oscillation (ENSO) may be the primary driver inducing drought in Southeast Asia (Malhi & Wright 2004). Furthermore, results from a global climate model showed more frequent El Niño-like conditions because of the human-induced greenhouse effect (Timmermann *et al*. 1999).

Bornean tropical rainforests in Southeast Asian tropics are among the moistest biomes of the world, with abundant rainfall throughout the year (see fig. 3 in Kumagai *et al*. 2005). In these climatic conditions, there is intense water and carbon exchange between the atmosphere and the forest ecosystem (Kumagai *et al*. 2004c, 2005, 2009). This also implies that small perturbations in the rainfall regime could significantly change biogeochemical cycling; for example, a severe drought was associated with the ENSO event of 1997–1998, which induced high tree mortality in tropical rainforests of Malaysian and Indonesian Borneo (Nakagawa *et al*. 2000; van Nieuwstadt & Sheil 2005; Allen *et al*. 2010). Thus, it is important to understand the drought physiology of rainforests adapted to very moist environments to predict how the dynamics of such forest ecosystems will respond to climate change (see Fisher *et al*. 2006).

In terms of regulation of water status, plants can be categorized as 'isohydric' or 'anisohydric'. This is thought to be a promising approach to define basic drought physiology, which can be used to quantify the causes of climate-induced forest dynamics, especially mortality and die-off (e.g. Fisher *et al*. 2006; Franks, Drake & Froend 2007; McDowell *et al*. 2008; Breshears *et al*. 2009). Isohydric plants regulate transpiration by stomatal closure to maintain constant midday leaf water potential, thus avoiding drought-induced hydraulic failure. However, stomatal closure during longer periods of drought can lead to carbon starvation, resulting in tree mortality (McDowell *et al*. 2008; Breshears *et al*. 2009). In contrast, anisohydric plants have less stomatal sensitivity and allow midday leaf water potential to decline with decreasing soil moisture. Thus, hydraulic failure occurs at a much more negative water potential for anisohydric than for isohydric species (e.g. Linton, Sperry & Williams 1998; West *et al*. 2007). This may help anisohydric species to stave off carbon starvation at least during moderate but long droughts. Some studies have suggested that anisohydric

Correspondence: T. Kumagai. E-mail: tomoomikumagai@gmail.com

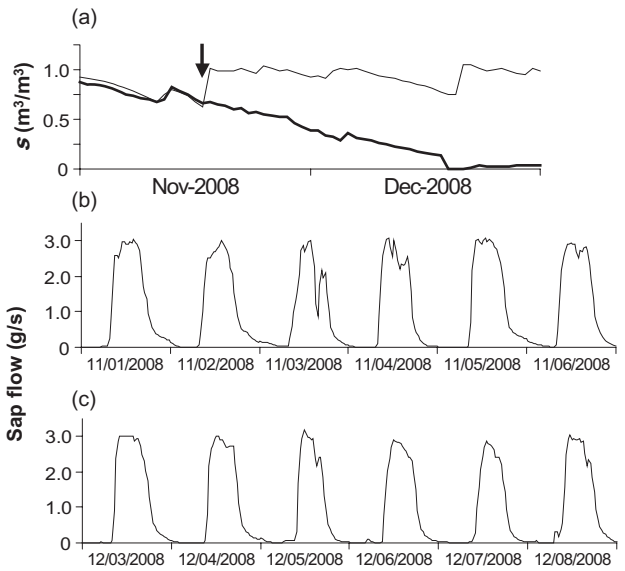

Figure 1. Time series of soil moisture (s) at the through-fall exclusion experiment site (thick line) and a control site (thin line) (a), and diurnal courses of whole-tree (*Dryobalanops aromatica* Gaertn. f.) sap flow under normal conditions (b) and severe drought conditions (c). Arrow denotes start of experiment. There was little change in sap flow between normal and severe drought conditions.

species tend to have xylem morphology adapted to withstand lower water potential without excessive and catastrophic cavitation, and that regulation allows these species to continue to take up carbon during severe drought (Oren *et al*. 1999; Ewers *et al*. 2005; McDowell *et al*. 2008). Anisohydric plants have been reported to occupy more drought-prone habitats than isohydric species, although there are exceptions (see McDowell *et al*. 2008). In effect, several aspects of the environmental or evolutional significance and mechanisms of both isohydric and anisohydric species remain unclear (Franks *et al*. 2007).

Previous studies (Kumagai *et al*. 2004c, 2005) and our on-going through-fall exclusion experiment (Fig. 1) indicate that the studied tropical rainforest ecosystem, which is normally a very moist environment, tends to have little regulation of forest water use, even during the sporadic periods of severe soil drying. It is interesting to note that the 50 cm top soil layer at this study site, comprising sandy clay loam, can retain around 70 mm water even under residual soil moisture conditions (Kumagai *et al*. 2004b,c); therefore, during periods of severe drought, transpiration of this rainforest might continue using the soil water. Thus, we hypothesized that anisohydric behaviour would confer a carbon uptake advantage to tree species adapted to the moist environment, because there would be little risk of water stress-induced hydraulic failure (see Kumagai *et al*. 2008). In this study, we clarified and tested the above hypothesis, and suggest a reason why anisohydric plants may be prevalent at the studied tropical rainforest site. We analysed the effects of climate-induced water stress on water status, productivity and survival of both isohydric and anisohydric plant species, and discuss their advantages in a given environment. We then tested the potential critical point of the presence of anisohydric plants in response to a global-change-type drought (see Breshears *et al*. 2005).

METHODS

Soil moisture dynamics is a key factor controlling hydrologic fluxes through the soil–plant–atmosphere continuum (SPAC). Thus, soil moisture dynamics can be fundamental information for describing ecosystem processes such as water stress and carbon assimilation (e.g. Rodriguez-Iturbe *et al*. 1999; Laio *et al*. 2001; Porporato *et al*. 2001; Porporato, Daly & Rodriguez-Iturbe 2004; Rodriguez-Iturbe & Porporato 2004). Accounting only for changes in mean responses to climatic variability is not sufficient for realistic investigations on the effects of climate change on ecosystems. Instead, such investigations must account for the stochastic component of hydrologic forcing and its possible changes in terms of frequency and amount of rainfall events. These changes are responsible for modifying soil moisture dynamics and the temporal structure (i.e. intensity, duration and frequency) of periods of water stress and impaired plant assimilation (Porporato *et al*. 2001, 2004). Probabilistic descriptions of ecosystem process dynamics are useful to describe the effects of climatic fluctuations such as severe drought induced by current ENSO cycles and global climate change.

In this study, we used a simple SPAC model linked to probabilistic descriptions of soil moisture and plant water stress (Porporato *et al*. 2001), to arrive at a synthetic characterization of plant carbon assimilation dynamics (Daly, Porporato & Rodriguez-Iturbe 2004). The computed results were linked to previous observations in a tropical rainforest in Southeast Asia (Kumagai *et al*. 2004a,b,c, 2005, 2006; Manfroi *et al*. 2006; Ohashi *et al*. 2008). We compared the dynamics of plant water stress and productivity between isohydric and anisohydric species in various rainfall regimes. We used a stochastic representation to test their advantages and survival in the studied tropical rainforest site under the current climatic conditions and under possible climate change-induced drought. For completeness, a review and description of the modelling scheme is presented in the following discussion (see Rodriguez-Iturbe & Porporato 2004) and a list of symbols used in the model is given in the Appendix.

Stochastic soil moisture dynamics model

The stochastic soil moisture model used in this study was originally proposed by Rodriguez-Iturbe *et al*. (1999) and improved by Laio *et al*. (2001). Under the conditions that lateral movement can be neglected, the vertically integrated soil moisture balance equation is given as follows:

$$nZ_r \frac{ds(t)}{dt} = R(t) - I(t) - Q[s(t),t] - E[s(t),t] - L[s(t)] \qquad (1)$$

where n is the soil porosity, Z_r is the rooting depth, s is the degree of saturation varying between 0 and 1, t is time, R is the rainfall rate, I is the canopy interception loss, Q is the rate of infiltration-excess, $E(s, t)$ is the evapotranspiration rate and $L(s)$ is the leakage. Equation 1 is a stochastic ordinary differential equation for the state variable s, and is solved on daily timescales. The frequency of rainfall events can be assumed to be a stochastic variable expressed as an exponential distribution with the mean time interval between precipitation events $1/\lambda$. The amount of rainfall, when it occurs, is also assumed to be an independent random variable described by an exponential probability distribution with the mean depth of rainfall events, α. Losses to the atmosphere from canopy interception, I, are represented using a threshold of rainfall depth Δ, which denotes interception capacity and below which effectively no water reaches the ground. Saturation overland flow, Q, is derived from rainfall excess, which occurs when rainfall depth exceeds the available storage.

Leakage losses are assumed to occur through gravitational flow. $L(s)$ is assumed to be at its maximum for saturated soil moisture conditions and can be expressed as the hydraulic conductivity $K(s)$, that is, the exponential function of K_{sat}, the saturated hydraulic conductivity, s_{fc}, s at 'field capacity', the water content held in the soil after gravity drainage where $K(s)$ has a value of zero, and β, a parameter that can be obtained by fitting the power law unsaturated hydraulic conductivity to the field data (e.g. Laio *et al*. 2001).

In this model, the main limiting factor controlling the evapotranspiration is considered to be soil moisture. Specifically, the dependence on s is given by (e.g. Laio *et al*. 2001)

$$E(s,t)=\begin{cases} 0, & \text{for} \quad 0<s(t)\le s_h \\ E_W\dfrac{s(t)-s_h}{s_W-s_h}, & \text{for} \quad s_h<s(t)\le s_W \\ E_W+(E_{max}-E_W)\dfrac{s(t)-s_W}{s^*-s_W}, & \text{for} \quad s_W<s(t)\le s^* \\ E_{max}, & \text{for} \quad s^*<s(t)\le 1 \end{cases} \tag{2}$$

where E_W and E_{max} are the soil evaporation and the maximum evapotranspiration, respectively, and s_h, s_W and s^* are s at 'hygroscopic point', 'plant wilting point' and 'plant stress point', respectively. When s falls below a given s^*, plant transpiration is reduced by stomatal closure to prevent internal water losses. Then, soil water availability becomes a key factor in determining the actual evapotranspiration rate. Transpiration and root uptake continue at a reduced rate until s reaches s_W. Below s_W, soil water is further depleted only by evaporation at a low rate to s_h.

When the soil contribution to total evaporation is insignificant (given the high leaf area index, LAI, at the site) and in the absence of free water on vegetation, the bulk surface conductance is strongly related to the behaviour of leaf stomatal conductance (Kelliher *et al*. 1995; Raupach 1995, 1998). Equilibrium evaporation occurs when air passes over an extensive wet surface and becomes saturated. However, because even such air is seldom saturated, the ratio of actual evaporation to the equilibrium evaporation is often 20–30% greater than unity (Priestley & Taylor 1972). This ratio is referred as the Priestley–Taylor coefficient, α_{PT}. De Bruin (1983) found that although α_{PT} varies with wind speed, surface roughness, and the entrainment of dry air at the top of the atmospheric boundary layer, it depends primarily on the surface conductance. Furthermore, McNaughton & Jarvis (1983) showed that equilibrium evaporation is the evaporation at the limit of complete decoupling. In our previous studies (Kumagai *et al*. 2004c, 2005), we found high decoupling coefficient values because of the relatively large surface conductance compared with aerodynamic conductance, and that net available energy is the primary forcing variable for evapotranspiration at the study site. Thus, we used a modified Priestley & Taylor (1972) expression to compute E_W and E_{max}, as follows:

$$E_i=\kappa\alpha_{PT\_i}\frac{\delta}{L_v\rho_w(\delta+\varepsilon)}R_n \tag{3}$$

where i denotes W or max, α_{PT_W} and α_{PT_max} are the Priestley–Taylor coefficients (α_{PT}) for E_W and E_{max}, respectively, κ is a unit conversion factor, δ is the rate of change of saturation water vapour pressure with temperature, L_v is the latent heat of vapourization of water, ρ_w is the density of water, ε is the psychrometric constant, and R_n is the net radiation above the canopy. A major uncertainty in Eqn 3 is α_{PT}, which, for forested ecosystems, is usually less than its typical value of 1.26 because of additional boundary layer, leaf, xylem and root resistances. Measured evapotranspiration data are used to obtain daily α_{PT}, and then the relationship between s and daily α_{PT} can be derived. α_{PT_W} and α_{PT_max} are parameterized by fitting Eqns 2 and 3 to the relationship (see Fig. 2a). For the stochastic model computations, all thermodynamic variables in Eqn 3 were assumed to be constant values, R_n was also obtained by averaging yearly observed values, and the effect of atmospheric humidity on stomatal conductance was ignored to maintain analytical tractability. Note that using averaged R_n (which gave an averaged value of evapotranspiration; Kumagai *et al*. 2004b, 2009), and using a function for stomatal response to increasing vapour pressure deficit (Kumagai *et al*. 2004a,b) resulted in little change to the probabilistic descriptions of soil moisture and daily transpiration rate. Figure 2a summarizes the evapotranspiration model used in this study.

Because of the stochastic rainfall forcing in Eqn 1, its solution can be represented only in a probabilistic manner. In this framework, the probability density function (PDF) of s, $p(s)$, can be derived from the master equation of the process (see Rodriguez-Iturbe & Porporato 2004).

Carbon assimilation and plant water stress dynamics

Daily carbon assimilation A_n is defined as the canopy photosynthetic rate, which does not take into consideration the

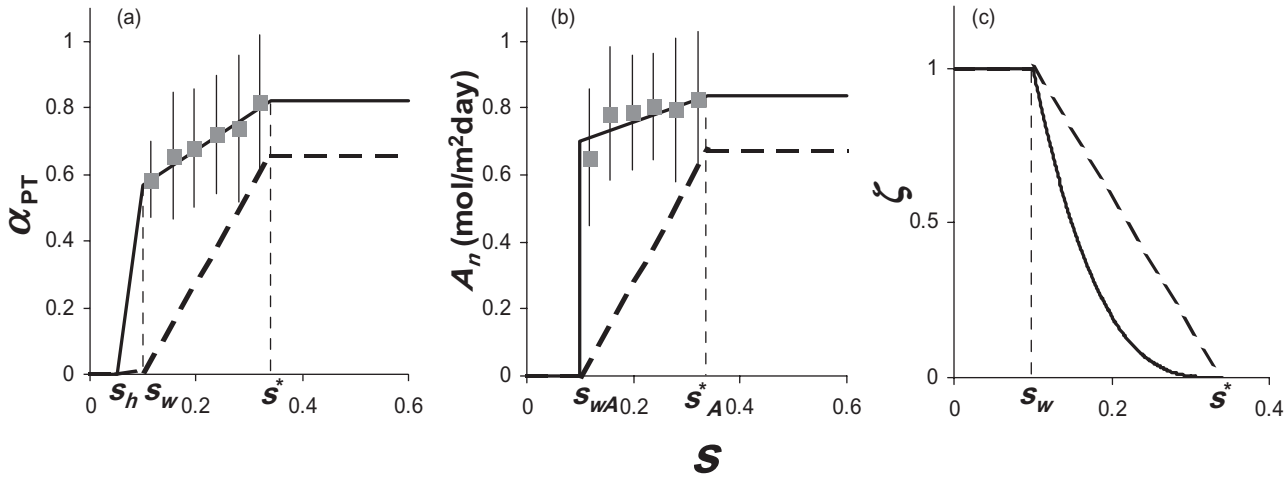

Figure 2. Relationships between soil moisture (s) and (a) transpiration (Priestley–Taylor coefficient, α_{PT}), (b) carbon assimilation (A_n), and (c) static water stress (ζ), for anisohydric (solid lines) and isohydric (broken lines) species. Closed squares denote eddy covariance measured α_{PT} and A_n in bins of s, and vertical bars represent one standard deviation. The parameters used for soil characteristics are $s_h = 0.05$, $s_W = s_{WA} = 0.1$, $s^* = s^*_A = 0.34$, and those for transpiration, carbon assimilation and static water stress are $\alpha_{PT\_W} = 0.57$ and 0.01, $\alpha_{PT\_max} = 0.82$ and 0.66, $A_W = 0.7$ and 0 mol m^{-2} day^{-1}, $A_{max} = 0.84$ and 0.67 mol m^{-2} day^{-1}, and $q = 3$ and 1 for anisohydric and isohydric species, respectively.

carbon lost by ecosystem respiration. A behaviour similar to that of $E(s, t)$ is also found for the dependence of A_n on s (see Fig. 2a,b). This dependence may be functionally approximated as follows (Daly *et al.* 2004):

$$A_n(s,t) = \begin{cases} 0, & \text{for} \quad s(t) \le s_{WA} \\ A_W + (A_{max} - A_W)\dfrac{s(t) - s_{WA}}{s^*_A - s_{WA}}, & \text{for } s_{WA} < s(t) \le s^*_A \\ A_{max}, & \text{for} \quad s^*_A < s(t) \end{cases} \tag{4}$$

where s_{WA} and s^*_A are s_W and s^* for assimilation, respectively, and A_W and A_{max} are A_n at s_{WA} and the maximum value, respectively. The probabilistic structure of A_n can be derived from $p(s)$ by a derived-distribution approach. Accordingly, the PDF of A_n, $p(A_n)$, has an atom of probability in zero, $P_{A0} = \int_0^{s_{WA}} p(s)ds$; one in A_{max}, $P_{Amax} = \int_{s^*_A}^1 p(s)ds$; and is continuous in between. In this study, the mean assimilation during a season, $\langle A_n \rangle = \int_0^{A_{max}} A_n p(A_n) dA_n$, is used to analyse productivity of isohydric and anisohydric plant species in each given climatic condition.

Following Porporato *et al.* (2001) the (static) plant water stress, ζ, can be defined as zero when soil moisture is above the level of incipient stomatal closure, s^*, and defined as the maximum value of one when soil moisture is at the level of complete stomatal closure, s_W. There is a non-linear curve in the value of ζ between s^* and s_W:

$$\zeta(t) = \begin{cases} 1, & \text{for} \quad s(t) \le s_W \\ \left[\dfrac{s^* - s(t)}{s^* - s_W}\right]^q, & \text{for} \quad s_W < s(t) \le s^*, \\ 0, & \text{for} \quad s^* < s(t) \end{cases} \tag{5}$$

where q is a measure of the non-linearity of the effect of soil moisture deficit on plant conditions, and can vary with plant species (Fig. 2c). Plants with a higher q-value, that is, stronger non-linearity, can have lower ζ with decreasing s but abruptly increase ζ in the immediate vicinity of s_W. This means that such plants can allow their leaf water potential to approach the xylem cavitation threshold without suffering from water stress (Porporato *et al.* 2001).

Like in the case of $p(A_n)$, the probabilistic structure of ζ can be derived from $p(s)$ by substituting Eqn 5 for s. The PDF of ζ, $f_Z(\zeta)$, has an atom of probability at $\zeta = 0$, $F_Z(0) = 1 - P(s^*)$, and one at $\zeta = 1$ equal to $F_Z(1) = P(s_W)$ (where P denotes the cumulative density function of s). The continuous part of $f_Z(\zeta)$ between zero and one corresponding to $s_W < s < s^*$ can be written as follows (Porporato *et al.* 2001):

$$f_Z(\zeta) = \frac{C_\zeta}{\xi_W}\left[\left(1 - \frac{\xi}{\xi_W}\right)\zeta^{\frac{1}{q}} + \frac{\xi}{\xi_W}\right]^{\lambda\frac{s^* - s_W}{\xi - \xi_W} - 1} \exp\left\{\mu\left[(s^* - s_W)\zeta^{\frac{1}{q}} - s^*\right]\right\} \tag{6}$$

in which

$$\xi_W = \frac{E_W}{nZ_r}, \quad \xi = \frac{E_{max}}{nZ_r}, \quad \mu = \frac{nZ_r}{\alpha}, \tag{7}$$

where C_ζ is an integration constant, which can be found by imposing the condition $F_Z(0) + F_Z(1) + \int_0^1 f_Z(\zeta)d\zeta = 1$.

The mean water stress can be calculated as $\bar{\zeta} = \int_0^1 \zeta f_Z(\zeta)d\zeta + F_Z(1)$. However, as the value of $\bar{\zeta}$ also takes into consideration the periods of $\zeta = 0$, we consider

the mean value of water stress given that, for our purposes, the plant is under stress (Porporato *et al*. 2001):

$$\bar{\zeta}' = \frac{\bar{\zeta}}{P(s^*)} \tag{8}$$

where $P(s^*)$ denotes only the part of the PDF corresponding to ζ above 0.

The information on plant conditions given by the mean and the PDF of water stress needs to be completed by describing the duration of the period of water stress. The length of the time in which soil moisture is below a threshold is among the most important stochastic variables to analyse the temporal dimension of water stress. The analytical expression for the mean duration of an excursion below the threshold, s_w, can be obtained using a crossing analysis as follows (Porporato *et al*. 2001):

$$\overline{T_{sw}} = \frac{1}{\lambda'} + \frac{1}{\lambda'}[\mu(s_w - s_h)]^{-\lambda'\frac{s_w - s_h}{\xi_w}} \gamma\left[1 + \lambda'\frac{s_w - s_h}{\xi_w}, \mu(s_w - s_h)\right] \exp[\mu(s_w - s_h)] \tag{9}$$

where λ' is the frequency of rainfall events given by $\lambda\exp(-\Delta/\alpha)$, and $\gamma[\cdot,\cdot]$ is the lower incomplete gamma function.

Porporato *et al*. (2001) defined the measure of vegetation water stress combining $\bar{\zeta}'$ with the mean duration and frequency of water stress during the growing season, known as 'dynamic' water stress or mean total dynamic stress during the growing season, $\bar{\theta}$. Likewise, to describe plant mortality and survival induced by hydraulic failure under severe drought conditions, here we defined a 'tree death index', η, using Eqns 8 and 9 as follows:

$$\eta = \begin{cases} \dfrac{\bar{\zeta}'\overline{T_{sw}}}{kT_{seas}} & \text{if} \quad \bar{\zeta}'\overline{T_{sw}} < kT_{seas}, \\ 1 & \text{otherwise}, \end{cases} \tag{10}$$

where k is a parameter representing an index of plant resistance to drought and T_{seas} is the length of a growing season. Tree mortality described by η was related to a permanent damage caused by drought-induced hydraulic failure. Note that, unlike Porporato *et al*.'s $\bar{\theta}$, we use $\overline{T_{sw}}$ instead of using the mean duration of an excursion below s^*. Moreover, we do not take into account the effect of the frequency of water stress in Eqn 10 because permanent damage leading to tree mortality occurs at the maximum level of water stress and tree mortality is a single event. In this study, the tree death index during a season, η, is used to analyse plant mortality and survival of isohydric and anisohydric species in each given climatic condition.

THE DATA

Vegetation–atmosphere exchange and meteorological data, which were well suited for estimating the SPAC model parameters, were obtained for a natural forest in Lambir Hills National Park (LHNP; 4°12′N, 114°02′E, 200 m a.s.l.) 30 km south of Miri City, Sarawak, Malaysia. The rainforest in LHNP consists of two types of original vegetation common to Borneo; mixed dipterocarp and tropical heath forest. The former contains various genera of the family Dipterocarpaceae, which covers 85% of LHNP. The average canopy height in the study site is approximately 40 m, but the heights of the emergent treetops can reach 50 m. The LAI ranged spatially from 4.8 to 6.8 $m^2 m^{-2}$ with a mean of 6.2 $m^2 m^{-2}$. The monthly amounts of litterfall were similar throughout the year, suggesting only small variations in the LAI. The soils consist of red-yellow podzolic soils (Malaysian classification) or ultisols (United States Department of Agriculture Soil Taxonomy), with high sand content (62–72%), an accumulation of nutrients at the surface horizon, low pH (4.0–4.3) and high porosity (54–68%).

The mean annual rainfall (Θ) at Miri Airport, 20 km from LHNP, was approximately 2740 mm for the period from 1968 to 2001. In LHNP, the value was approximately 2600 mm for the period from 2000 to 2006. The long-term record at Miri Airport shows significant inter-annual variations in rainfall in this region; for example, the maximum and minimum annual rainfalls for 1968–2001 were 3499 mm in 1988 and 2125 mm in 1976, respectively. In the computations used in this study, we used default parameters for rainfall characteristics, which were estimated from the above long-term record and $\Theta = T_{seas}\lambda\alpha$, as $\Theta = 2740$ mm, $\lambda = 0.54$ day^{-1} and $\alpha = 13.9$ mm. The mean annual temperature in LHNP is approximately 27 °C with little seasonal variation.

In LHNP, we established a 4 ha experimental plot gridded into 400 subplots of 10×10 m. An 80 m tall (at the base of the gondola) canopy crane with a 75 m long rotating jib was constructed at the centre of this plot to provide access to the upper canopy. Some observational floors of the canopy crane were devoted to eddy-covariance flux measurements and above-canopy meteorological measurements such as radiation flux, air temperature and humidity, wind velocity and rainfall. The subplots were used for measurements of through-fall, stemflow, in-canopy micrometeorological factors, and soil moisture.

Table 1 shows the model parameters for soil characteristics and evapotranspiration for computing the soil moisture dynamics in LHNP. The methods by which these parameters were derived and how the computation results were validated are provided elsewhere (Kumagai *et al*. 2009). Note

Table 1. Model parameters of soil characteristics and evapotranspiration in Lambir Hills National Park

Parameter	Description	Value
Z_r (mm)	Eqn 1	1000
n	Eqn 1	0.36
K_{sat} (mm day^{-1})	Saturated hydraulic conductivity	33.4
β	Exponent of the soil–water retention curve	6.3
R_n (W m^{-2})	Eqn 3	135.3
Δ (mm)	Interception capacity	1.10

that although R_n data were separated for wet and dry seasons in Kumagai *et al*. (2009), yearly average R_n was used in this study because the distinction between wet and dry seasons is somewhat unclear in LHNP. In the present study, we used the eddy covariance measured evapotranspiration and net ecosystem exchange (see Kumagai *et al*. 2004a, 2006) to derive the relationships between s and daily α_{PT} (Kumagai *et al*. 2004b) and A_n for the vegetation, that is, anisohydric plants (Fig. 2a,b). It should be noted that these α_{PT} and A_n functions of s in Fig. 2a,b are highly consistent with observed results; that is, the tropical rainforest ecosystem in LHNP shows little regulation of forest water use despite episodic severe soil drying.

The α_{PT} and A_n for isohydric plants were assumed to increase linearly from ~0 at s_w to their maximum values at s^* and then remain constant to saturation (Fig. 2a,b). In addition, isohydric plants are assumed to be more parsimonious than the anisohydric plants, because isohydric plants lose their high gas exchange ability in compensation for their economical water use. Isohydric plants regulate stomatal aperture to prevent water potential from falling below a critical threshold (see McDowell *et al*. 2008), and this corresponds to the assumed relationship between α_{PT} and s. Also, Franks & Farquhar (1999) showed that reduced stomatal sensitivity to atmospheric dryness is accompanied by higher gas exchange capacity. This finding lends support to our assumption about the different behaviour of A_n in response to s between isohydric and anisohydric plants: first, the maximum values of α_{PT} (α_{PT_max}) and A_n (A_{max}) for isohydric plants were arbitrarily set at 80% of those for anisohydric plants (Fig. 2a,b). Then, we examined the sensitivity of productivity to changing α_{PT_max} and A_{max} in isohydric plants. Given the above difference in the α_{PT} functions of s between isohydric and anisohydric plants, the increment rate of ζ with soil moisture deficit can be taken as a constant increase for isohydric plants, and a non-linear increase for anisohydric plants (Fig. 2c). This assumption is thought to be reasonable because anisohydric plants can allow their water potential to approach the hydraulic failure threshold without sensing water stress (see McDowell *et al*. 2008). In the same manner as the sensitivity test to changing the α_{PT_max} and A_{max} in isohydric plants, first, we arbitrarily set the non-linearity parameter in Eqn 5, q, as 3 (Fig. 2c), and then examined the sensitivity of mortality to changing q in anisohydric plants.

Nakagawa *et al*. (2000) reported extremely high tree mortality at this study site as a result of the severe drought associated with the ENSO event of 1997–1998. We determined the parameters of plant resistance to drought, k, in Eqn 10 for both plant types, assuming that the tree death index, η, reaches its maximum value under such severe hydroclimatic conditions (see Kumagai *et al*. unpublished data).

Using the model parameters for the present vegetation, that is, anisohydric plants, and time courses of rainfall as local forcing data, the soil moisture balance model (Eqn 1) was validated in deterministic mode (i.e. not using probabilistic descriptions). As a result, we found that the model well reproduced the structure of measured s time series (Fig. 3) (Kumagai *et al*. 2009). Also, in the context of the s model validation, we confirmed that the modelled estimates of total annual evapotranspiration and carbon assimilation were consistent with the measured values (see Kumagai *et al*. 2004a, ~1400 mm year^{-1} and ~33 tC ha^{-1} year^{-1}, respectively).

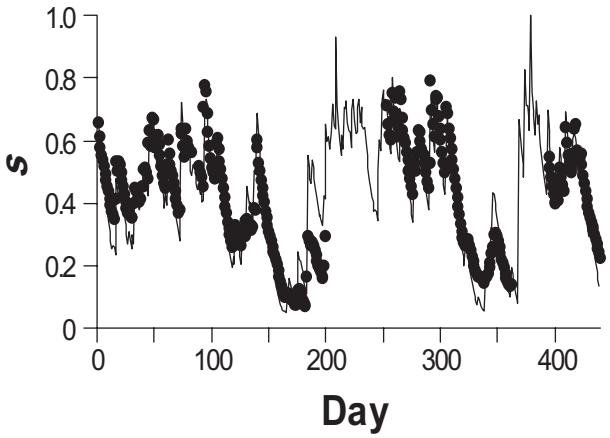

Figure 3. Time series of measured (solid circles) and calculated (curve) daily average soil moisture content (s) in Lambir Hills National Park. The measurement period was day of year (DOY) 78, 2001 to DOY 151, 2002.

RESULTS

Figure 4a and b show the mean assimilation, $\langle A_n \rangle$, of anisohydric and isohydric plants (using 80% values of the maximum α_{PT} (α_{PT_max}) and A_n (A_{max}) for anisohydric plants), respectively, as a function of the frequency of rainfall events (λ) with total rainfall (Θ) kept constant. The productivity of anisohydric plants was high and constant for $\Theta > 1300$ mm, but decreased below this value (Fig. 4a). On the other hand, isohydric plant productivity remained relatively stable with varying Θ, despite its significant decrease when $\Theta < 1100$ mm (Fig. 4b). Also, changes in $\langle A_n \rangle$ of isohydric plants with varying λ were less than those of anisohydric plants, and this tendency was apparent below Θ = approximately 1100 mm (Fig. 4a,b). Differences in $\langle A_n \rangle$ between anisohydric and isohydric plants (Fig. 4c) revealed that the productivity of anisohydric plants was higher than that of isohydric plants for any rainfall regime as long as $\Theta > 1100$ mm, and that the productivity of isohydric plants surpassed that of anisohydric plants at any (realistic) λ-value below Θ = approximately 800 mm. As a further analysis, we plotted λ at $\langle A_n \rangle_a - \langle A_n \rangle_i = 0$ (λ_0: see Fig. 4c) against Θ to identify the transition zone between the relative merits of the anisohydric and isohydric plants' productivities (Fig. 5). The relationship between Θ and λ_0 was approximately linear within a narrow range (Θ = 840 to 1060 mm), implying that there may be an abrupt transition of the predominance of one species over another as the rainfall regime changes.

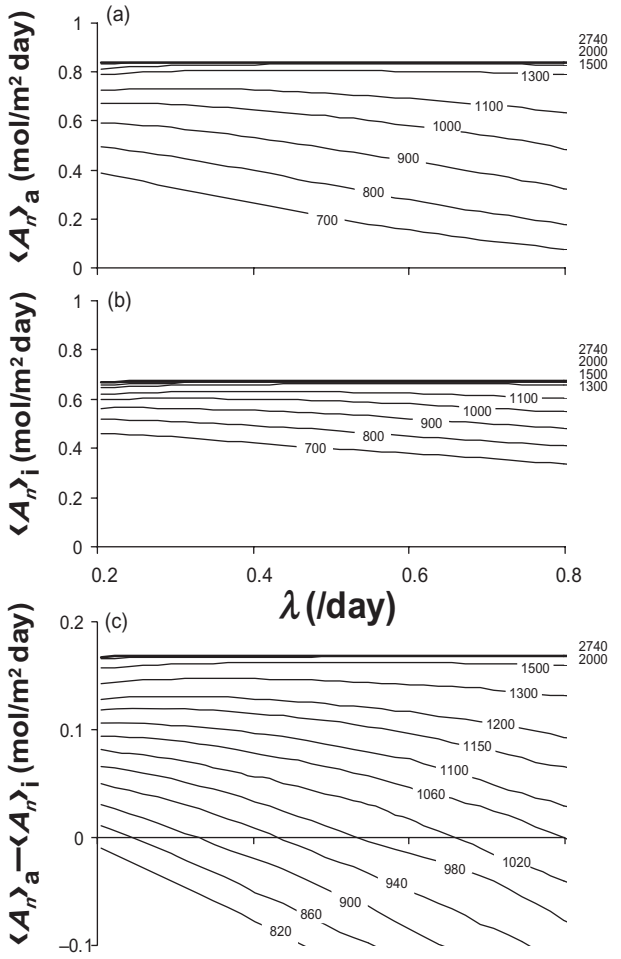

Figure 4. Mean assimilation rate ($\langle A_n \rangle$) computed for anisohydric (a) and isohydric plants (b) (represented by subscripts a and i, respectively) and their difference (c) as a function of frequency of rainfall events (λ) for different annual total rainfall (represented by the number (mm) on or beside each line).

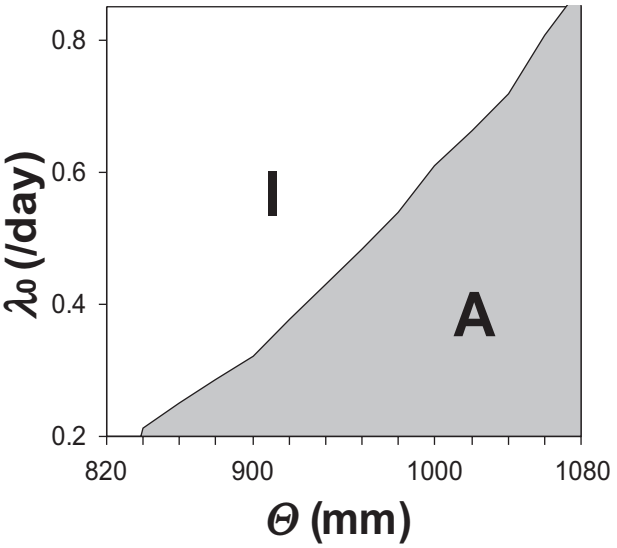

Figure 5. Annual total rainfall (Θ) versus the frequency of rainfall events (λ) when $\langle A_n \rangle$ of anisohydric plants is equal to $\langle A_n \rangle$ of isohydric plants (λ_0: see Fig. 2c). A and I denote regions where productivity of anisohydric plants surpasses that of isohydric plants, and vice versa, respectively.

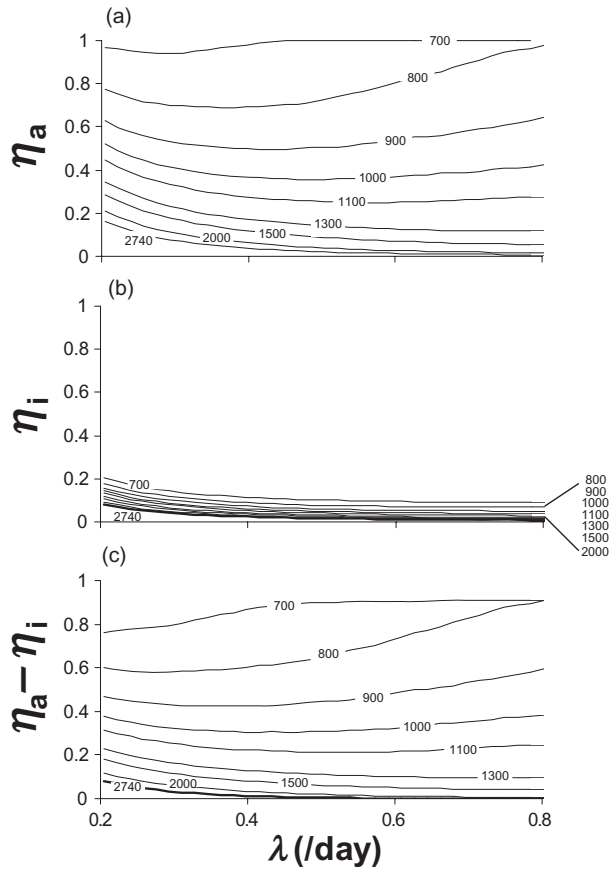

Figure 6. Tree death index (η) computed for anisohydric (a) and isohydric plants (b) (represented by subscripts a and i, respectively) and their difference (c) as a function of frequency of rainfall events (λ) for different annual total rainfall (represented by the number (mm) on or beside each line).

Likewise, we compared the tree death index (η) as a function of λ between anisohydric (using the non-linear parameter $q = 3$) and isohydric plants (Fig. 6). Decreasing Θ markedly increased the hydraulic failure-induced mortality of anisohydric plants (Fig. 6a), but not isohydric plants (Fig. 6b). An increase in λ denotes conditions of frequent but low rainfall intensity. Under such conditions, anisohydric plants above Θ = approximately 1200 mm (Fig. 6a) and isohydric plants for any Θ (Fig. 6b) decrease their risk of hydraulic failure and mortality, whereas for anisohydric plants under drier conditions there are 'optimum' values of λ that minimize their mortality (Fig. 6a). In the absence of drought (i.e. above Θ = approximately 1500 mm), normal mortality rates are likely to be lower for both types of plants, but under drier conditions (below Θ = approximately 1000 mm), isohydric plants tended to survive and prevent hydraulic failure more effectively than anisohydric plants (Fig. 6c).

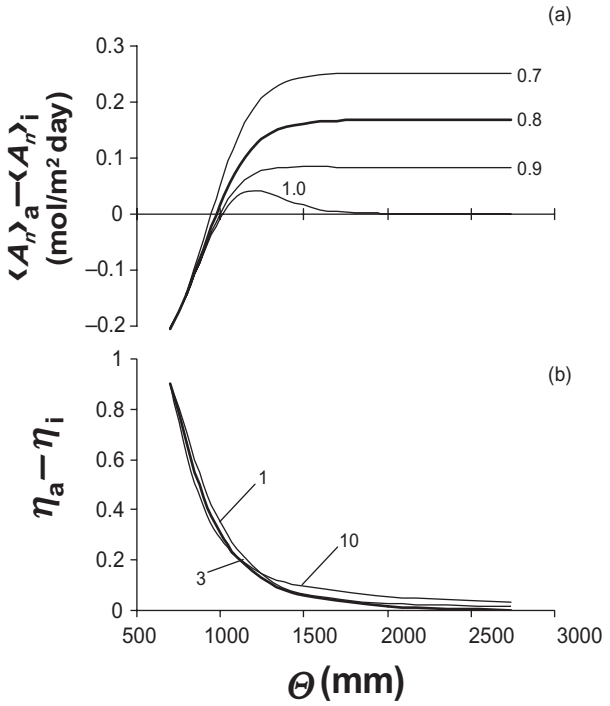

Figure 7. Differences in mean assimilation rate ($\langle A_n\rangle_a - \langle A_n\rangle_i$; a) and tree death index ($\eta_a - \eta_i$; b) between anisohydric and isohydric plants as functions of annual total rainfall (Θ) for a given frequency of rainfall events ($\lambda = 0.54$ day^{-1}). Lines represent different values of α_{PT_max} and A_{max} (a) and q (b), as indicated by numbers alongside. Numbers in A represent conversion factors used to multiply anisohydric plants' α_{PT_max} and A_{max} to obtain corresponding values for isohydric plants.

Figure 7 shows differences in $\langle A_n\rangle$ and η between anisohydric and isohydric plants when λ is kept constant as the default value ($\lambda = 0.54$ day^{-1}) but mean depth of the rainfall event (α) and Θ are changed. In addition, we investigated the effects of changing model parameters α_{PT_max} and A_{max} for isohydric plants and q for anisohydric plants on productivity (Fig. 7a) and mortality (Fig. 7b), respectively. When using parameters less than approximately 90% of α_{PT_max} and A_{max}, anisohydric plants showed much higher productivity than isohydric plants at approximately $\Theta > 1300$ mm (Fig. 7a). Even when the same values for α_{PT_max} and A_{max} were used for the two plant types, the difference in $\langle A_n\rangle$ was greater than zero, peaking at approximately $\Theta = 1200$ mm (Fig. 7a). However, using any q for anisohydric plants, the mortality of the two types of the plants was the same at approximately $\Theta > 1300$ mm (Fig. 7b). This implies that in this area, including the study site with $\Theta = 2740$ mm, anisohydric plants tend to occur naturally. On the other hand, at $\Theta = 1000$ mm, although there is no advantage in productivity for anisohydric plants (Fig. 7a), their mortality becomes appreciably higher than that of isohydric plants (Fig. 7b). Furthermore, below this Θ, using any values for the parameters, isohydric plants showed greater productivity and lower mortality than anisohydric plants (Fig. 7a,b). This may indicate the prevalence of isohydric plants in areas where $\Theta < 1000$ mm.

DISCUSSION

Partitioning isohydric and anisohydric species might be an effective approach for modelling climate change-induced forest dynamics that affect plant survival and mortality under severe drought conditions. McDowell *et al.* (2008) provided a general framework for the hypothetical mechanisms underlying tree mortality: carbon starvation occurs when the duration of the drought and the resulting reduction in photosynthesis exceed the amount of carbon reserves stored for maintenance of metabolism, whereas hydraulic failure occurs if the drought is sufficiently intense to push a plant past its threshold for irreversible desiccation before carbon starvation occurs.

This categorization, when the stomatal regulation characteristics of isohydric and anisohydric species are taken into account, implies that the main cause of mortality of isohydric species is carbon starvation, and that of anisohydric species is hydraulic failure. Some research has documented, at least partially, the validity of this hypothesis (e.g. Breshears *et al.* 2009). Likewise, in our computations, the higher productivity of anisohydric species under relatively wet conditions (Figs 4 & 7) might indicate that anisohydric species are more resistant than isohydric species to carbon starvation.

In our model, we used the function of tree mortality considering only hydraulic failure. This was because for isohydric and anisohydric species, mortality caused by carbon starvation depends on impairment of photosynthesis by water stress and is thus closely related to xylem hydraulic failure. Furthermore, there is recent evidence that avoiding the risk of hydraulic failure is the best strategy for water use in both isohydric and anisohydric species. For example, McDowell (2011) reported feedback between hydraulic conductivity and carbohydrate availability, and Meinzer *et al.* (2009) reported a variety of mechanisms for maintaining hydraulic safety under dynamic conditions.

Our model suggests that anisohydric species may be more susceptible than isohydric species to drought-related mortality induced by hydraulic failure (Figs 6 & 7). However, it has been reported that in general, anisohydric plants are better adapted to drier environments because of their more cavitation-resistant xylem (Oren *et al.* 1999; Clearwater & Clark 2003; Brodribb & Holbrook 2004; Ewers *et al.* 2005; McDowell *et al.* 2008). A notable insight that emerges from the adaptation of anisohydric species to drought-prone habitats is that such anisohydric plants are likely to have lower s_w and higher q (see Fig. 2c). This is because their xylem structure confers morphological advantages, allowing leaf water potential to approach its cavitation threshold without incurring damage from the xylem hydraulic failure (see Porporato *et al.* 2001). Instead, their α_{PT_max} accompanied by A_{max} (see Fig. 2a,b)

is likely to be reduced because of the positive relationship between gas exchange capacity and its insensitivity to environmental factors (e.g. Franks & Farquhar 1999). Note that α_{PT} and A_n at the lower s domain (see Fig. 2a,b) are still greater for anisohydric than isohydric plants. For this case, we computed $\langle A_n \rangle$ and η for both types of plants; under drier conditions, $\langle A_n \rangle$ became higher and η became lower for anisohydric plants, compared with their respective values for isohydric plants. This implies that anisohydric species may be prevalent in drought-prone habitats (data not shown).

Figure 7 shows the possible prevalence of anisohydric species at the studied rainforest site in the wetter domain ($\Theta > 1000$ mm). It is important to note that we assumed no seasonality in rainfall in these computations (see Kumagai *et al*. 2005). The reduction in Θ is likely to be accompanied by a prolonged dry period, which affects plants' strategies to cope with soil water availability (Rodriguez-Iturbe *et al*. 2001). For example, Fisher *et al*. (2006) conducted a through-fall exclusion experiment in an Eastern Amazonian rainforest, shifting the rainfall regime toward that of a seasonal forest or savanna bioclimatic zone. They found that the plants used for their through-fall exclusion experiment were isohydric, implying an exception to our computed results. Furthermore, Malhi *et al*. (2009) pointed out that in considering the transient response of the rainforest to rapid climate change, there may be some buffers against drought, which are attributed to isohydric regulation of forest water use observed in the Eastern Amazonian rainforest (Fisher *et al*. 2007). These possible discrepancies with our results are likely because of the fact that, although the mean annual rainfall in their rainforest is comparable with that at our site (around 2300 mm), the pronounced dry season between July and December gives an advantage to isohydric behaviour. In reality, some studies, including a finding from the control plot of the through-fall exclusion experiment (Fisher *et al*. 2006), found no seasonality in transpiration. This implies, at least partly, that there is anisohydric regulation of water use in an Amazonian (Carswell *et al*. 2002) and a Bornean (Fig. 1; Kumagai *et al*. 2004c, 2005) tropical rainforest, suggesting the possible existence of anisohydric plants in these moist environments.

In summary, distinguishing between isohydric and anisohydric species might be critical when considering forest dynamics, because the preferential mortality of isohydric/anisohydric species in response to severe drought may alter the composition of the vegetation (e.g. Mueller *et al*. 2005). The framework presented in this study allows us to consider the effects of different physiological characteristics of isohydric or anisohydric species on their responses to changes in hydroclimatic variables, and consequently, to determine the effects of such changes on forest dynamics (see Porporato *et al*. 2004). This, however, will require more extensive and technically difficult experiments to understand the physiology of rainforest trees, and how they respond to both sporadic and new (i.e. climate change-induced) severe drought events.

ACKNOWLEDGMENTS

T.K. is grateful to the Forestry Department, Sarawak, for their support during the fieldwork for this study. T.K. also thanks Tohru Nakashizuka, Masakazu Suzuki and Tetsukazu Yahara for their support and numerous colleagues for their help with fieldwork, especially Natsuko Yoshifuji, Tomonori Kume, Makiko Tateishi and Kenji Tsuruta. We thank Stefano Manzoni for his valuable comments. This study was funded by Core Research for Evolutional Science and Technology (CREST) of the Japan Science and Technology Agency (JST), the Global COE (Centers of Excellence) Program (GCOE) of the Japan Society for the Promotion of Science (JSPS), grants from the Ministry of Education, Science and Culture, Japan (nos. 20380090 and 19255006) and the Excellent Young Researcher Overseas Visit Program under the sponsorship of the JSPS.

REFERENCES

Allen C.D., Macalady A.K., Chenchouni H., *et al*. (2010) A global overview of drought and heat-induced tree mortality reveals emerging climate change risk for forests. *Forest Ecology and Management* **259,** 660–684.

Breshears D.D., Cobb N.S., Rich P.M., *et al*. (2005) Regional vegetation die-off in response to global-change-type drought. *Proceedings of the National Academy of Sciences of the United States of America* **102,** 15144–15148.

Breshears D.D., Myers O.B., Meyer C.W., Barnes F.J., Zou C.B., Allen C.D., McDowell N. & Pockman W.T. (2009) Tree die-off in response to global change-type drought: mortality insights from a decade of plant water potential measurements. *Frontiers in Ecology and Environment* **7,** 185–189.

Brodribb T.J. & Holbrook N.M. (2004) Diurnal depression of leaf hydraulic conductance in a tropical tree species. *Plant, Cell & Environment* **27,** 820–827.

Carswell F.E., Costa A.L., Palheta M., *et al*. (2002) Seasonality in CO_2 and H_2O flux at an eastern Amazonian rain forest. *Journal of Geophysical Research* **107**. doi:10.1029/2000JD000284.

Clearwater M.J. & Clark C.J. (2003) In vivo magnetic resonance imaging of xylem vessel contents in woody lianas. *Plant, Cell & Environment* **26,** 1205–1214.

Daly E., Porporato A. & Rodriguez-Iturbe I. (2004) Coupled dynamics of photosynthesis, transpiration, and soil water balance. Part II: Stochastic analysis and ecohydrological significance. *Journal of Hydrometeorology* **5,** 559–566.

De Bruin H.A.R. (1983) A model for the Priestley-Taylor parameter α. *Journal of Climate and Applied Meteorology* **22,** 572–578.

Ewers B.E., Gower S.T., Bond-Lamberty B. & Wang C.K. (2005) Effects of stand age and tree species on canopy transpiration and average stomatal conductance of boreal forests. *Plant, Cell & Environment* **28,** 660–678.

Fisher R.A., Williams M., do Vale R.L., da Costa A.L. & Meir P. (2006) Evidence from Amazonian forests is consistent with isohydric control of leaf water potential. *Plant, Cell & Environment* **29,** 151–165.

Fisher R.A., Williams M., Lola da Costa A., Malhi Y., da Costa R.F., Almeida S. & Meir P. (2007) The response of an Eastern Amazonian rain forest to drought stress: results and modelling analyses from a throughfall exclusion experiment. *Global Change Biology* **13,** 2361–2378.

Franks P.J. & Farquhar G.D. (1999) A relationship between humidity response, growth form and photosynthesis operating point in C-3 plants. *Plant, Cell & Environment* **22,** 1337–1349.

Franks P.J., Drake P.L. & Froend R.H. (2007) Anisohydric but isohydrodynamic: seasonally constant plant water potential gradient explained by stomatal control mechanism incorporating variable plant hydraulic conductance. *Plant, Cell & Environment* **30,** 19–30.

Houghton R.A. & Hackler J.L. (1999) Emissions of carbon from forestry and land-use change in tropical Asia. *Global Change Biology* **5,** 481–492.

Kanae S., Oki T. & Musiake K. (2001) Impact of deforestation on regional precipitation over the Indochina Peninsula. *Journal of Hydrometeorology* **2,** 51–70.

Kelliher F.M., Luening R., Raupach M.R. & Schulze E.-D. (1995) Maximum conductances for evaporation from global vegetation types. *Agricultural and Forest Meteorology* **73,** 1–16.

Kumagai T., Katul G.G., Porporato A., Saitoh T.M., Ohashi M., Ichie T. & Suzuki M. (2004a) Carbon and water cycling in a Bornean tropical rainforest under current and future climate scenarios. *Advances in Water Resources* **27,** 1135–1150.

Kumagai T., Katul G.G., Saitoh T.M., Sato Y., Manfroi O.J., Morooka T., Ichie T., Kuraji K., Suzuki M. & Porporato A. (2004b) Water cycling in a Bornean tropical rain forest under current and projected precipitation scenarios. *Water Resources Research* **40**. doi:10.1029/2003WR002226.

Kumagai T., Saitoh T.M., Sato Y., Morooka T., Manfroi O.J., Kuraji K. & Suzuki M. (2004c) Transpiration, canopy conductance and the decoupling coefficient of a lowland mixed dipterocarp forest in Sarawak, Borneo: dry spell effects. *Journal of Hydrology* **287,** 237–251.

Kumagai T., Saitoh T.M., Sato Y., Takahashi H., Manfroi O.J., Morooka T., Kuraji K., Suzuki M., Yasunari T. & Komatsu H. (2005) Annual water balance and seasonality of evapotranspiration in a Bornean tropical rainforest. *Agricultural and Forest Meteorology* **128,** 81–92.

Kumagai T., Ichie T., Yoshimura M., Yamashita M., Kenzo T., Saitoh T.M., Ohashi M., Suzuki M., Koike T. & Komatsu H. (2006) Modeling CO_2 exchange over a Bornean tropical rain forest using measured vertical and horizontal variations in leaf-level physiological parameters and leaf area densities. *Journal of Geophysical Research* **111**. doi:10.1029/2005JD006676.

Kumagai T., Aoki S., Shimizu T. & Otsuki K. (2008) Transpiration and canopy conductance at two slope positions in a Japanese cedar forest watershed. *Agricultural and Forest Meteorology* **148,** 1444–1455.

Kumagai T., Yoshifuji N., Tanaka N., Suzuki M. & Kume T. (2009) Comparison of soil moisture dynamics between a tropical rainforest and a tropical seasonal forest in Southeast Asia: impact of seasonal and year-to-year variations in rainfall. *Water Resources Research* **45**. doi:10.1029/2008WR007307.

Laio F., Porporato A., Ridolfi L. & Rodriguez-Iturbe I. (2001) Plants in water-controlled ecosystems: active role in hydrologic processes and response to water stress. II. Probabilistic soil moisture dynamics. *Advances in Water Resources* **24,** 707–723.

Linton M.J., Sperry J.S. & Williams D.G. (1998) Limits to water transport in Juniperus osteosperma and Pinus edulis: implications for drought tolerance and regulation of transpiration. *Functional Ecology* **12,** 906–911.

Mabuchi K., Sato Y. & Kida H. (2005) Climatic impact of vegetation change in the Asian tropical region. Part I. Case of the Northern Hemisphere summer. *Journal of Climate* **18,** 410–428.

McDowell N.G. (2011) Mechanisms linking drought, hydraulics, carbon metabolism, and vegetation mortality. *Plant Physiology* **155,** 1051–1059.

McDowell N., Pockman W.T., Allen C.D., *et al*. (2008) Mechanisms of plant survival and mortality during drought: why do some plants survive while others succumb to drought? *New Phytologist* **178,** 719–739.

McNaughton K.G. & Jarvis P.G. (1983) Predicting effects of vegetation changes on transpiration and evaporation. In *Water Deficits and Plant Growth*, Vol. **V** (ed. T.T. Kozlowski), pp. 1–48. Academic Press, New York, USA.

Malhi Y. & Grace J. (2000) Tropical forests and atmospheric carbon dioxide. *Trends in Ecology and Evolution* **15,** 332–337.

Malhi Y. & Wright J. (2004) Spatial patterns and recent trends in the climate of tropical rainforest regions. *Transactions of the Royal Society of London. Series B, Biological Sciences* **359,** 311–329.

Malhi Y., Aragao L.E.O.C., Galbraith D., Huntingford C., Fisher R., Zelazowski P., Sitch S., McSweeney C. & Meir P. (2009) Exploring the likelihood and mechanism of a climate-change-induced dieback of the Amazon rainforest. *Proceedings of the National Academy of Sciences of the United States of America* **106,** 20610–20615.

Manfroi O.J., Kuraji K., Suzuki M., Tanaka N., Kume T., Nakagawa M., Kumagai T. & Nakashizuka T. (2006) Comparison of conventionally observed interception evaporation in a 100-m^2 subplot with that estimated in a 4-ha area of the same Bornean lowland tropical forest. *Journal of Hydrology* **329,** 329–349.

Meinzer F.C., Johnson D.M., Lachenbruch B., McCulloh K.A. & Woodruff D.R. (2009) Xylem hydraulic safety margins in woody plants: coordination of stomatal control of xylem tension with hydraulic capacitance. *Functional Ecology* **23,** 922–930.

Mueller R.C., Scudder C.M., Porter M.E., Trotter R.T.I., Gehring C.A. & Whitham T.G. (2005) Differential tree mortality in response to severe drought: evidence for long-term vegetation shifts. *Journal of Ecology* **93,** 1085–1093.

Nakagawa M., Tanaka K., Nakashizuka T., *et al*. (2000) Impact of severe drought associated with the 1997–1998 El Niño in a tropical forest in Sarawak. *Journal of Tropical Ecology* **16,** 355–367.

van Nieuwstadt M.G.L. & Sheil D. (2005) Drought, fire and tree survival in a Borneo rain forest, East Kalimantan, Indonesia. *Journal of Ecology* **93,** 191–201.

Ohashi M., Kumagai T., Kume T., Gyokusen K., Saitoh T.M. & Suzuki M. (2008) Characteristics of soil CO_2 efflux variability in an aseasonal tropical rainforest in Borneo Island. *Biogeochemistry* **90,** 275–289.

Oren R., Sperry J.S., Katul G.G., Pataki D.E., Ewers B.E., Phillips N. & Schäfer K.V.R. (1999) Survey and synthesis of intra- and interspecific variation in stomatal sensitivity to vapour pressure deficit. *Plant, Cell & Environment* **22,** 1515–1526.

Porporato A., Laio F., Ridolfi L. & Rodriguez-Iturbe I. (2001) Plants in water-controlled ecosystems: active role in hydrologic processes and response to water stress. III. Vegetation water stress. *Advances in Water Resources* **24,** 725–744.

Porporato A., Daly E. & Rodriguez-Iturbe I. (2004) Soil water balance and ecosystem response to climate change. *American Naturalist* **164,** 625–632.

Priestley C.H.B. & Taylor R.J. (1972) On the assessment of surface heat flux and evaporation using large-scale parameters. *Monthly Weather Review* **100,** 81–92.

Raupach M.R. (1995) Vegetation-atmosphere interaction and surface conductance at leaf, canopy and regional scales. *Agricultural and Forest Meteorology* **73,** 151–179.

Raupach M.R. (1998) Influences of local feedbacks on land-air exchanges of energy and carbon. *Global Change Biology* **4,** 477–494.

Rodriguez-Iturbe I. & Porporato A. (2004) *Ecohydrology of Water-Controlled Ecosystems: Soil Moisture and Plant Dynamics*. Cambridge University Press, New York, USA.

Rodriguez-Iturbe I., Porporato A., Ridolfi L., Isham V. & Cox D.R. (1999) Probabilistic modelling of water balance at a point: the role of climate, soil and vegetation. *Proceedings of the Royal Society of London. Series A. Mathematical and Physical Sciences* **455,** 3789–3805.

Rodriguez-Iturbe I., Porporato A., Laio F. & Ridolfi L. (2001) Intensive or extensive use of soil moisture: plant strategies to cope with stochastic water availability. *Geophysical Research Letters* **28,** 4495–4497.

Timmermann A., Oberhuber J., Bacher A., Esch M., Latif M. & Roeckner E. (1999) Increased El Niño frequency in a climate model forced by future greenhouse warming. *Nature* **398,** 694–697.

Werth D. & Avissar R. (2005) The local and global effects of Southeast Asian deforestation. *Geophysical Research Letters* **32**. doi:101029/2005GL022970.

West A.G., Hultine K.R., Jackson T.L. & Ehleringer J.R. (2007) Contrasting hydraulic strategies explain differential summer moisture use of Pinus edulis and Juniperus osteosperma. *Tree Physiology* **27,** 1711–1720.

World Resources Institute (2007) EarthTrends: Environmental Information. http://earthtrends.wri.org.

Received 7 January 2011; received in revised form 8 September 2011; accepted for publication 12 September 2011

APPENDIX

List of symbols

Symbol	Units	Definition
A_n	mol m^{-2} day^{-1}	Carbon assimilation rate
$\langle A_n \rangle$	mol m^{-2} day^{-1}	Mean assimilation during a season
A_W, A_{max}	mol m^{-2} day^{-1}	A_n at wilting point and the maximum value, respectively
C_ζ		Constant in Eqn 6
E	mm day^{-1}	Evapotranspiration rate
E_W, E_{max}	mm day^{-1}	Soil evapouration and maximum evapotranspiration, respectively
$f_Z(\zeta)$		Probability density function of static plant water stress, ζ
$F_Z(0)$, $F_Z(1)$		Atom of probability of static plant water stress, ζ at $\zeta = 0$ and 1, respectively
I	mm day^{-1}	Canopy interception loss
k		Index of plant resistance to drought
K	mm day^{-1}	Hydraulic conductivity
K_{sat}	mm day^{-1}	Saturated hydraulic conductivity
L	mm day^{-1}	Leakage rate
L_v	J kg^{-1}	Latent heat of vapourization of water
n	m^3 m^{-3}	Soil porosity
P		Cumulative density function of soil moisture, s
$p(A_n)$, $p(s)$		Probability density function of A_n and soil moisture, s, respectively
P_{A0}, P_{Amax}		Atom of probability of A_n in zero and A_{max}, respectively
q		Non-linearity of the effect of soil moisture deficit on plant conditions
Q	mm day^{-1}	Rate of infiltration-excess
R	mm day^{-1}	Rainfall rate
R_n	W m^{-2}	Net radiation above canopy
s	m^3 m^{-3}	Soil moisture as degree of saturation
s_{fc}, s_h, s_W, s^*	m^3 m^{-3}	s at field capacity, hygroscopic point, plant wilting point and plant stress point, respectively
s_{WA}, s^*_A	m^3 m^{-3}	s_W and s^* for assimilation, respectively
t	day	Time
T_{seas}	day	Length of a growing season
$\overline{T_{s_W}}$	day	Mean duration of an excursion below s_W
Z_r	mm	Rooting depth
α	mm	Mean depth of rainfall event
α_{PT_W}, α_{PT_max}		Priestley–Taylor coefficients, α_{PT}, for E_W and E_{max}, respectively
β		Exponent of the soil–water retention curve
Δ	mm	Interception capacity
δ	Pa K^{-1}	Rate of change of saturation water vapour pressure with temperature
ε	Pa K^{-1}	Psychrometric constant
ζ		Static plant water stress
$\bar{\zeta}$		Mean water stress during a season
$\bar{\zeta}'$		Mean water stress given that the plant is under stress
η		Tree death index
Θ	mm year^{-1}	Mean annual rainfall
$\bar{\theta}$		Mean total dynamic stress during a season
κ	mm s m^{-1} day^{-1}	Unit conversion factor
λ	day^{-1}	Mean rate of arrival of rainfall event
λ'	day^{-1}	Frequency of rainfall event taking into consideration canopy interception
μ		Constant in Eqn 6
ξ, ξ_W		Constant in Eqn 6
ρ_w	kg m^{-3}	Density of water